Comparative study on the overall energy performance between photovoltaic and Low-E insulated glass units

Jinqing Peng[1,2], Dragan C. Curcija[2*], Anothai Thanachareonkit[2], Eleanor S. Lee[2], Howdy Goudey[2], Jacob Jonsson[2], Stephen E. Selkowitz[2]*

1 College of Civil Engineering, Hunan University, Changsha 410082, Hunan, China

2 Building Technology and Urban Systems Division, Lawrence Berkeley National Laboratory, 1 Cyclotron Road, Berkeley, CA 94720, USA

*Corresponding author: Tel.: +86 (731) 84846217, +1 (510) 495 2602;

Email address: jallenpeng@gmail.com (*Jinqing Peng*)

DCCurcija@lbl.gov (*Dragan C. Curcija*)

Abstract

A novel semi-transparent building integrated photovoltaic (BIPV) laminate was developed and introduced in this paper. It was produced by cutting standard mono-crystalline silicon solar cells into small strips and then making electrical connections between each strip before laminating the cells between two layers of glass. The overall energy performance and energy saving potential of the BIPV insulated glass unit (IGU) under real world conditions were identified through a side by side comparative study. Compared to the reference IGU, the BIPV IGU had lower solar heat gain coefficient (SHGC) but much higher U-factor. The average HVAC electricity saving of the BIPV IGU was about 10% relative to the reference IGU. Daylighting measurement and analysis were carried out to evaluate the trade-offs associated with the BIPV IGU between daylight, glare, and lighting energy use. The results indicated that the BIPV IGU is better than the reference IGU in reducing discomfort glare. However, if the most conservative viewpoint near the window is used for the assessment, a lower transmittance BIPV IGU is required to bring the overall discomfort levels below the perceptible level. Lastly, the net energy saving potential associated with the novel BIPV IGU was identified based on the power, thermal and daylighting performance. On average, the BIPV IGU saved 16.8% of the total electricity use of the room. Further studies and improvement on the energy conversion efficiency of solar cells, the optimal transmittance as well as the thermal properties would make this technology more energy-efficient and affordable.

Keywords: building integrated photovoltaic (BIPV), semi-transparent PV laminate, energy saving, daylighting performance, solar heat gain coefficient, visual comfort

1. Introduction

In 2010, 41% of total energy consumption, equivalent about 40 quadrillion British thermal units (Btu), was consumed in residential and commercial buildings in the U.S. Among the total energy consumed in buildings, space heating, cooling and lighting accounted for more than 50% [1]. Windows, as the main envelope element connecting outdoor and indoor environments, present a significant effect on the energy consumption of space heating, cooling and lighting, especially for modern high-rise buildings with large window to wall ratio (WWR). It was estimated by the Department of Energy (DOE) that 30% of the energy used to heat and cool all buildings in the U.S. was lost through inefficient windows, corresponding to a waste of 4.1 Quads[1] energy per year [2]. Also, it is well known that windows providing sufficient daylighting illuminance and appropriate glare control could also significantly reduce the artificial lighting energy use. Thus, there is no doubt that high efficient window technologies offer huge energy saving potentials for buildings.

According to the functions of windows, there are mainly three performance criteria to evaluate the thermal and daylighting performance of window systems. The first assessment criterion is solar heat gain coefficient (SHGC), which evaluates the amount of solar energy through the window. SHGC is a dimensionless number from zero to one that represents the fraction of solar energy incident on the exterior of a window and frame that is transmitted to the interior. Usually, the higher the SHGC, the larger the cooling energy use in summer. The second assessment criterion is the U-factor, which is associated with the space heating energy consumption in winter. The term of U-factor is defined as the rate of heat loss through a window assembly. The lower the U-factor, the greater the thermal insulating performance. The last assessment criterion is the visible light transmission (T_{vis}), which is related to evaluate the daylighting performance of windows. High visible light transmission could increase daylighting illuminance level and in consequence reduce artificial lighting energy use and improve the quality of lighting, while too much direct light transmission may cause discomfort glare. Thus, a trade-off between harvesting daylighting illuminance and controlling glare should be considered.

Guided by the above three criteria, many high-performance window technologies, such as insulated glass windows, inert gas filled windows, Low-E coating windows, chromogenic windows, and vacuum glazing windows, have been developed and utilized to improve the energy efficient and occupant comfort in recent years [3-8]. However, all these technologies can only reduce power consumption in a passive way such as reflecting solar irradiation or preventing heat gain and daylighting penetration. They cannot work in an active way via absorbing and

[1] 1 The term "Quad" is shorthand for 1 quadrillion (1015) Btu = 1.056 EJ.

converting solar energy into electricity just like building integrated photovoltaic windows (BIPV windows) do.

BIPV windows refer to the use of semi-transparent PV (STPV) laminates to substitute for conventional glazing to constitute window systems [9]. Compared to other advanced window technologies, the most significant advantage of BIPV windows lies in that they can actively and appropriately utilize the incident solar irradiation for power generation through photovoltaic effect, and at the same time regulate solar heat gain and control daylight glare by adjusting the transmittance of PV laminates. In another word, an optimally designed BIPV window can not only reduce additional solar heat gain and unwanted daylighting glare but also actively convert the part of undesirable and excessive incident solar energy into electricity rather than passively reflect or prevent it. To some extent, BIPV windows are characterized by both functions of building energy efficiency and distributed renewable power generation. Thus, they provide pretty good choices for high-rise office buildings which are characterized by large window area, high solar heat gain as well as big peak load. With the further improvement of energy conversion efficiency and reduction of costs, semi-transparent BIPV windows with customized sizes, patterns and colors would achieve a much better overall energy performance and economic returns in future.

Owing to the above-mentioned advantages, the energy performance of semi-transparent BIPV windows/facades has been extensively investigated, including the heat transfer mechanism and thermal performance[10-15], air conditioning load reduction and solar heat gain [16-23], thermal comfort [24,25], daylighting performance [26-32], annual thermal and electrical simulation [33-35], energy saving potential [36-38] and outdoor performance tests [39-42]. Through literature review, it was found that the transparency of STPV laminates used in BIPV windows was normally achieved by one of three design approaches. For the first thin-film PV approach, the deposited solar cell layer can be so thin that it supported some visible light transmission, but the transmittance was usually as low as 5%, which can't meet the desired daylighting requirement. The energy conversion efficiency of this kind of BIPV window is limited by the thin film technology and a typical value was less than 8%. Laser cut technology was introduced in the second thin-film PV approach, in which thin-film solar cell layers was cut away and patterned by a laser cut process to increase the transparency. Theoretically, any visible transmittance can be achieved with this approach by adjusting the cut area of solar cells. However, the energy conversion efficiency would be lower than 10% if the high transmittance is desired. For the third approach, transparency was achieved by capturing a patterned array of opaque crystalline silicon (c-Si) solar cells between the layers of a laminate with the desired interval of unobstructed space between the cells, such that there was light transmission between the cells. The energy conversion efficiency of this kind of BIPV window depends on the transmittance. Taking the BIPV window with 30% transmittance as an example, its energy conversion efficiency can be as high as 15%. However, patterned STPV laminates with large opaque crystalline solar cells (156x156 mm^2) will likely disrupt the view of building occupants and result in visual discomfort.

In summary, both the existing semi-transparent thin-film PV laminates and the crystalline silicon PV laminates have advantages and disadvantages regarding energy conversion efficiency, appearance aesthetics and/or visual comfort. In this context, a novel STPV laminate was developed and introduced in this paper. This STPV laminate was produced by cutting standard crystalline silicon solar cells into narrow strips and then automatically welding and connecting the strips into strings for laminating. As this STPV laminate combined the advantages of both the laser groove thin-film PV laminates and the conventional c-Si STPV laminates, it not only possesses beautiful appearance and pretty good visual effect but also characterized by relatively high energy conversion efficiency. In addition, although much research related to the energy performance of STPV windows have been reported in recent years, the comparative experimental study of the overall energy efficiency between a semi-transparent BIPV window and a commonly used window was not found. In this paper, to evaluate the overall energy performance of the novel semi-transparent BIPV insulated glass unit (IGU) relative to a typical Low-E coated reference IGU, a side by side outdoor comparative test was conducted on FLEXLAB (Facility for Low Energy Experiment in Buildings) at Lawrence Berkeley National Laboratory (LBNL). Various energy consumption related parameters were measured during this test, including daylighting illuminance, lighting electricity use, air-conditioning cooling/heating water flow rate, as well as power generation from the BIPV IGU. The thermal properties of both the BIPV IGU and the Low-E reference IGU were measured and analyzed. Also, HVAC electricity uses of the both test cells equipped with the BIPV IGU and Low-E IGU were calculated respectively based on the measured cooling/heating water flow rate and the corresponding temperature difference. Lastly, the overall energy performance of the BIPV IGU was determined and its energy saving potential compared to the Low-E coating reference IGU was identified.

2. BIPV and Low-E insulated glass units

2.1 Semi-transparent BIPV laminate

The novel semi-transparent BIPV laminate studied in this paper was developed by Solaria Co. in the U.S. It was produced based on mono-Si standard solar cells, and the manufacturing processes can be summarized into four steps. Firstly, the mono-Si solar cells are produced and cut into strips with customizable width, spacing and length according to different applications and daylighting requirements. Secondly, the narrow solar cell strips are welded into PV strings automatically and then the strings are connected in series or parallel according to the required voltage and current. Thirdly, the connected PV strings are embedded in glasses and PVB layers for laminating. Lastly, the laminate is integrated with another glass sheet to form an insulated glass unit (IGU) to improve its thermal performance. The transmittance and energy conversion efficiency of this kind of PV laminate can be customized by changing the spacing of adjacent strips. Figure 1 presents the structure diagram of the Solaria semi-transparent PV laminate. The solar cell strings are embedded into glass lites and PVB layers during the laminating process.

PVB layers are used to protect the solar cell strings from the erosion of external environment, especially humidity, which could accelerate aging and deterioration of solar cells.

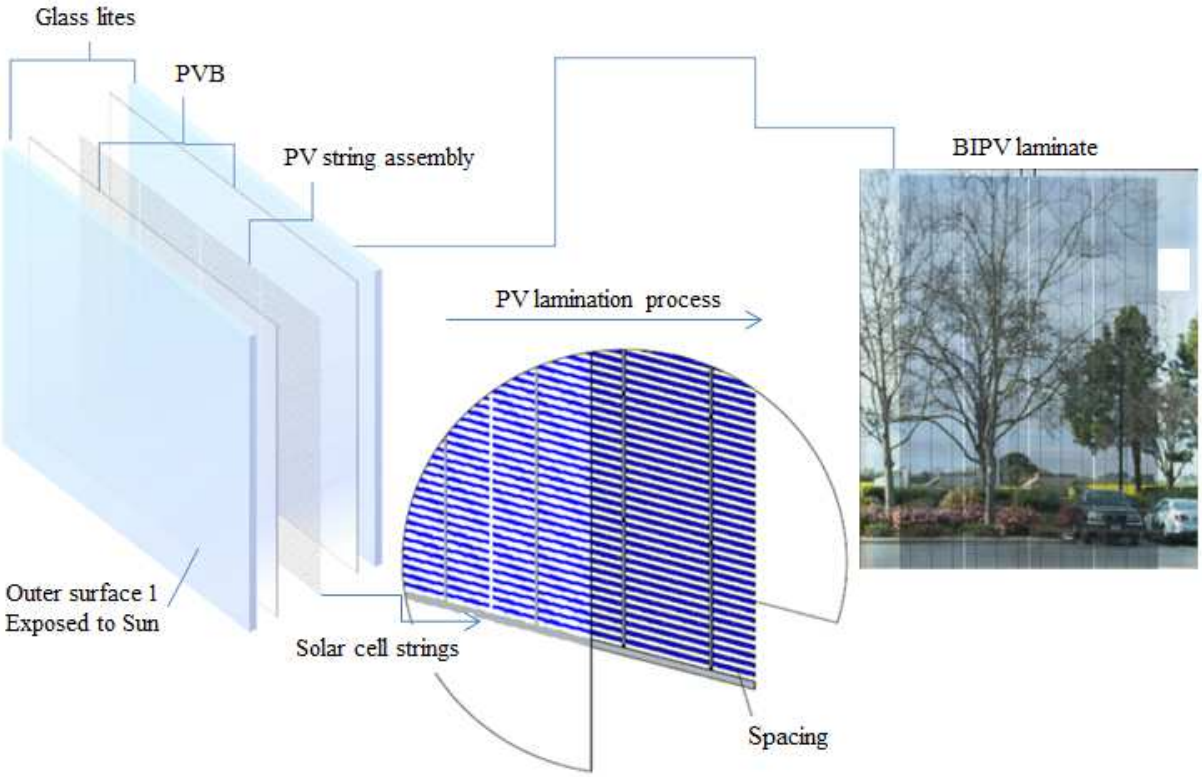

Figure 1 Construction diagram of Solaria BIPV laminate (Solaria report)

The electrical specifications of the semi-transparent BIPV laminate were measured under standard test conditions (STC, viz. solar irradiation 1000W/m^2, air mass 1.5 and module temperature 25℃), as shown in Table 1. The open circuit voltage, short circuit current, and maximum power output were 23.9 V, 7.6 A, and 137 W, respectively. The dimension of the BIPV laminate was 1448 mm ×1764 mm (W×H), but only one-third of the laminate was covered by solar cells. The energy conversion efficiency of the whole BIPV laminate under STC was measured to be 7%, which is much higher than that of thin-film based PV laminates with the same transmittance.

Table 1 Electrical specifications of the BIPV laminate under standard test conditions [43]

Electrical specifications under (STC)	
Maximum power output, (P_{max})	137 W
Open circuit voltage, (V_{oc})	23.9 V
Short circuit current, (I_{sc})	7.6 A
Voltage at the maximum power point, (V_{mp})	19.6 V
Current at the maximum power point, (I_{mp})	7.0 A
Fill factor	0.76

PV area efficiency, (η)	7%
Dimension, (mm)	1448×1764

2.2 BIPV insulated glass unit

Our previous study reported that due to both the high absorptivity and the high infrared emittance, the single panel PV laminates had a bad thermal insulation performance [38]. To improve the thermal insulation performance of single panel PV laminates, a glass sheet was adhered on the back side of the Solaria BIPV laminates to form a BIPV insulated glass unit (IGU). The schematic diagram of the BIPV IGU is illustrated in Figure 2. It consisted of an 11.25 mm BIPV outboard laminate, a 5 mm clear inboard glass lite and a 12 mm air gap. The BIPV laminate, from outside to inside, was constituted by 5mm Starphire lite/ 0.5 mm PVB interlayer/ 0.25 mm solar cell strings/ 0.5 mm PVB interlayer/ 5mm Starphire lite. The Solarban 70XL Low-E coating was deposited on the third surface to further improve its thermal performance.

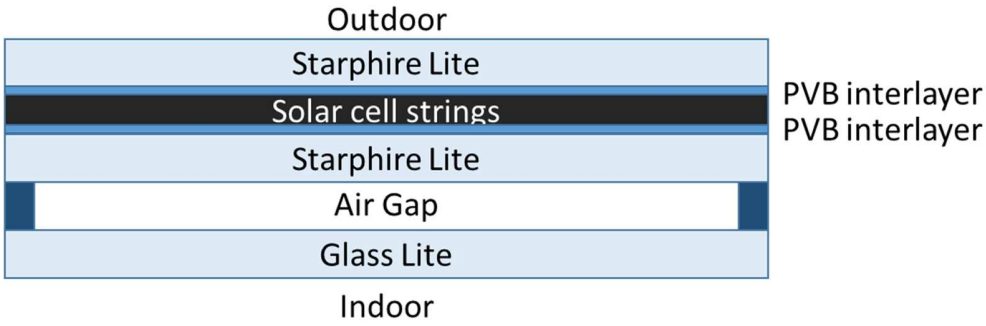

Figure 2 Schematic diagram of the Solaria BIPV IGU

2.3 Low-E coated insulated glass unit

To evaluate the energy saving potential of the BIPV IGU, a reference IGU, which not only represents the most common advanced technology available today but also has a similar structure with the BIPV IGU, was adopted for the comparative study. The schematic diagram of the reference IGU is illustrated in Figure 3. It is seen that the reference IGU stack is constituted by a 6 mm Starphire with Solarban 70XL outboard lite on a 6 mm clear inboard lite with 12 mm air gap. The total thickness is 24 mm, thinner than the BIPV IGU by 4.25 mm. It is worth noting that the Solarban 70XL Low-E coating was deposited on the second surface, facing to the air cavity, for the Low-E reference IGU, but it was deposited on the third surface, toward outside, for the BIPV IGU. The different placements of Low-E coating may result in different thermal insulation performance for these two IGUs.

Figure 3 Schematic diagram of the Low-E reference IGU

The thermal and optical properties of the reference IGU was simulated by the WINDOW 7.3 under the environmental conditions of NFRC 100-2010. Table 2 lists the calculated values. The solar heat gain coefficient, shading coefficient, and light transmittance are 0.275, 0.316 and 0.64, respectively. The U-factor in winter and summer are 1.62 and 1.55, respectively. It is seen that no matter the thermal properties or optical characteristics of the reference IGU are pretty good, and it represents the most popular advanced technology in building window industry.

Table 2 Simulated thermal and optical properties of the reference IGU

Properties	**Values**
U-factor (Winter) [W/m²K]	1.62
U-factor (Summer) [W/m²K]	1.55
Solar Heat Gain Coefficient [%]	27.5
Shading Coefficient [%]	31.6
Light Transmittance [%]	64
Solar Transmittance [%]	24.6
Solar Reflectance (inner) [%]	37.5
Solar Reflectance (outer) [%]	52.4
Solar Absorbance [%]	23.1

3. Facility for comparative test

3.1 Introduction of FLEXLAB

Facility for Low Energy Experiment in Buildings (FLEXLAB) at Lawrence Berkeley National Laboratory (LBNL), as shown in Figure 4, is the most flexible, comprehensive, and advanced building efficiency simulator in the world. FLEXLAB lets users test energy-efficient building systems individually or as an integrated system, under real-world conditions. FLEXLAB test beds can test HVAC, lighting, windows, building envelope, control systems, and plug loads, in

any combination. Users can test alternatives, perform cost-benefit analyzes, and ensure a building will be as efficient as possible before construction or retrofitting even begins. At last, FLEXLAB can also conduct a comparative study in real-world conditions for different building components and equipment, such as windows, building envelopes, HVAC, lighting systems, such that to identify the energy saving potential of emerging building technologies. The main objective of this comparative test is to determine the energy saving potential of the semi-transparent BIPV IGU relative to the representative Low-E coated IGU on buildings.

Figure 4 Facility for Low Energy Experiment in Buildings (FLEXLAB) at Berkeley Lab

FLEXLAB consists of four test beds, viz. X1, X2, X3 and XR. Each test bed includes two identical test cells, which are used for comparative study. For X1 to X3 test beds, the orientation is fixed to due south, but XR, where the test was conducted, is a rotatable test bed. It can clockwise rotate from the southeast orientation to north orientation, thus, it was used in this study to test the overall energy performance of the BIPV IGU under different orientations. Figure 5 presents the layout of the rotatable XR test bed. There are two identical test cells; the left one is designated as XRA, where the Solaria BIPV IGUs were installed; the right one is designated as XRB where the Low-E reference IGUs were installed for comparison.

To comprehensively evaluate and compare the energy performance of the BIPV IGU and the Low-E reference IGU, the following sensors were employed for measuring various energy-related parameters in the XR test bed:

- Built-in water flow meters measure heating and chilled water flows
- Built-in temperature sensors measure supply and return water temperatures in heating and chilled water loops

- Built-in velocity sensors measure air flow in supply and return ductworks
- Built-in temperature sensors measure supply and return air flow temperatures
- Portable window energy meter (PWEM) measures the solar heat gain coefficient (SHGC) and U-factor
- Pyranometers measure the vertical façade incident solar irradiation and solar transmittance
- Weather station measures horizontal global solar radiation, diffuse radiation, cloud coverage, dry bulb temperature, relative humidity, wind speed and wind direction
- Power meters measure electrical power produced by the Solaria BIPV IGUs and lighting energy use

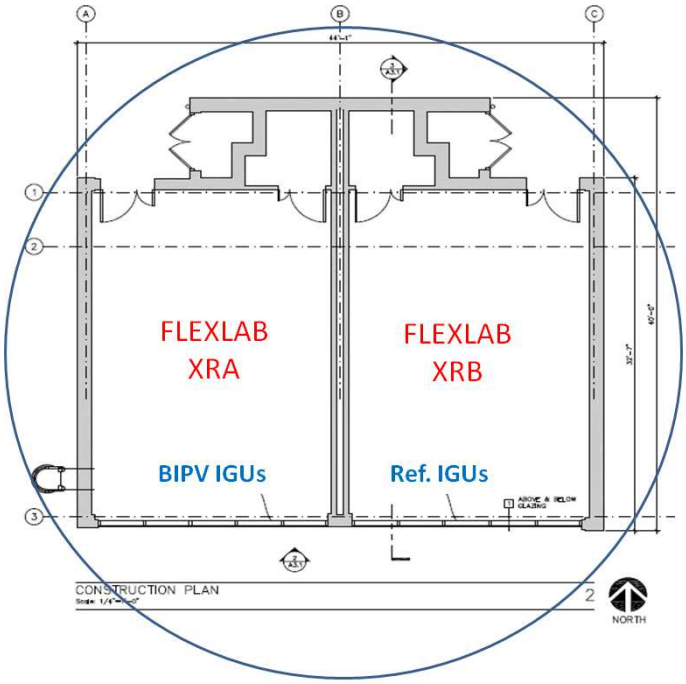

Figure 5 Layout of the rotatable XR test bed

The information of the sensors and their accuracies are listed in table 3.

Table 3 Information of the sensors and their accuracies

Instruments	Manufacturer	Technical data	Accuracy
Water flow meter	SITRANS F M MAG 3100	0 to 10 m/s	±0.2%
Temperature sensor	T type thermocouple	Temperature range: −50 to 400℃	±0.2℃
Air velocity sensor	Ebtron model	0 to 5000 fpm	±2%

	BTM116-PC		
Portable window energy meter (PWEM)	Self-made	Response time: 5 min	±0.05
Pyranometer	Eppley Model SPP	Spectral Range: 295 to 2800 nm Sensitivity: 8 μV/Wm^{-2} Response Time: 5 s	Measurement Uncertainty: approx. 2% (Hourly average) Calibration Uncertainty: <1%
Weather station	Self-made (Delta-T Sunshine Pyranometer SPN1-A990, BAPI BA/10K-2-O-BB, Gill 1590-PK-020)	Solar radiation: 0 to 2000W/m^2 Air DB temperature: -40 to 70 °C Air humidity: 0 to 95% RH Wind speed: 0 to 50 m/s	Solar radiation: ±5% Air DB temperature: ±0.1°C Air dew temperature: ±0.2°C Wind speed: ±1.5%
Power meter	Schneider	Current range: 0.15 to 20A	±2%

3.2 Installation & visual appearance

According to the opening size of the XR test bed, four pieces of BIPV IGUs were installed on the XRA cell. The total width and height of the BIPV IGUs were 5899.2 mm and 1828.8 mm, respectively. The total glazing area and active PV area were 9 m^2 and 3 m^2, respectively. The reference IGUs had the same layout and dimensions as the BIPV IGUs, and were installed on XRB cell for comparative testing. The real picture of these two IGUs is shown in Figure 6. The left one is the XRA test cell equipped with Solaria BIPV IGU; the right one is the XRB cell equipped with Low-E reference IGU. It is seen that there is almost no difference regarding outside appearance between BIPV IGU and reference IGU. Figures 7 and 8 show the views from inside to outside of the BIPV IGU and the reference IGU, respectively. As the existing of narrow solar cell strips in the laminate, the uniformity and visual effect of the BIPV IGU were worse than that of the reference IGU, which was constituted by low-iron clear glasses with Low-E coating. However, as shown in Figure 7, no matter the visual comfort or the daylighting performance of the BIPV IGU was largely acceptable especially when the merits of electricity generation and energy saving are taken into account.

Figure 6 Picture of the BIPV IGU and the reference IGU installed on the XR rotatable test bed

Figure 7 Inside to outside view of the BIPV IGU [43]

Figure 8 Inside to outside view of the reference IGU

4. Results and discussions

The side by side comparative test between the BIPV IGU and the reference IGU was conducted on the XR test bed from Sep. 30 to Dec.9, 2015. This test experienced different orientations, different set point temperatures as well as different blind shade positions such that to fully understand the electricity generation and energy saving potential of the BIPV IGU under different conditions. The energy-related parameters, including weather data, thermal properties of windows, HVAC electricity use, daylighting illuminance, lighting electricity use, glare probability, electrical power generation, were measured and recorded during the test. With the measured data, the overall energy performance including thermal, power and daylighting performance of the BIPV IGU was completely evaluated and analyzed.

4.1 Thermal properties

Compared to the reference IGU, the energy conversion and heat transfer processes of the BIPV IGU were more complicated. Solar energy absorbed by the solar cells is partly converted into electricity (only 15-17%) and the absorbed remainder, is dissipated as waste heat, resulting in a temperature increase of PV laminates. Figure 9 illustrates various surface temperature profiles of the BIPV IGU and the reference IGU. It is seen that the outer surface temperatures of both the

BIPV IGU and the reference IGU were very close, but the inner surface temperature of the BIPV IGU was higher than that of the reference IGU by 7 ℃ at noon.

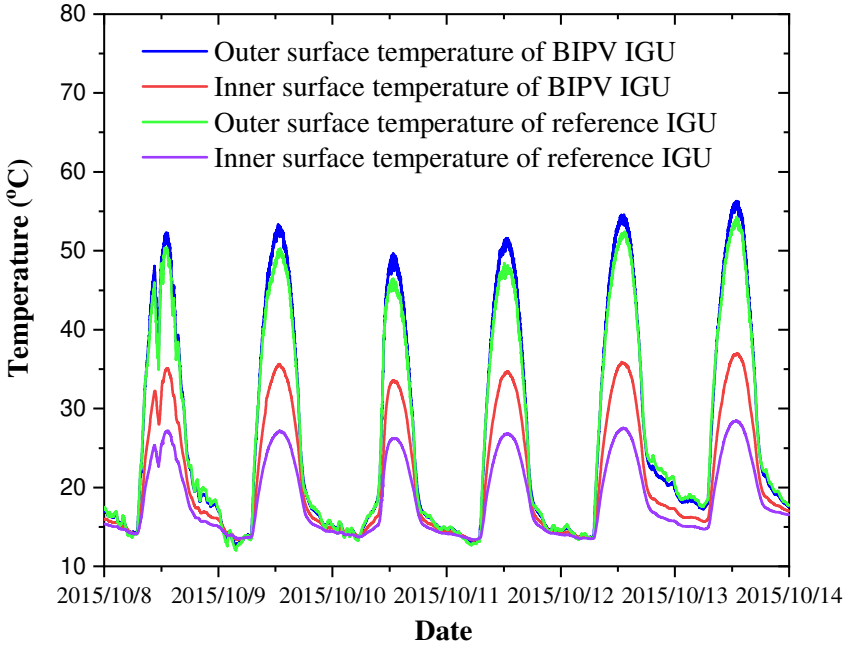

Figure 9 Comparison of surface temperatures between BIPV IGU and reference IGU

The solar heat gain coefficient (SHGC) and U-factor of both the BIPV IGU and the reference IGU were measured and compared. As shown in Figure 10, the BIPV IGU has lower SHGC than the reference IGU because the solar cells absorb and convert a portion of solar energy into electricity. The average SHGC of the BIPV IGU and the reference IGU were 0.25 and 0.32, respectively. Figures 11 and 12 present the U-factor of the BIPV IGU and the reference IGU, respectively. It is seen that the U-factor of the BIPV IGU is much higher than that of the reference IGU. The average U-factors of the BIPV and reference IGUs were 3.5 and 1.5, respectively. The main reason causing a significant difference of U-factor between the two kinds of IGUs was attributed to the different placement locations of Low-E coating. For the BIPV IGU, as mentioned before, the Low-E coating was deposited on the third surface with being embedded in the laminate. Thus, it cannot be fully effective to reflect longwave infrared radiation back to indoor rooms. If the Low-E coating is deposited on the fourth surface (facing to the indoor room) in future designs, the U-factor of the BIPV IGU would be reduced significantly, and its thermal insulation performance is expected to be improved further.

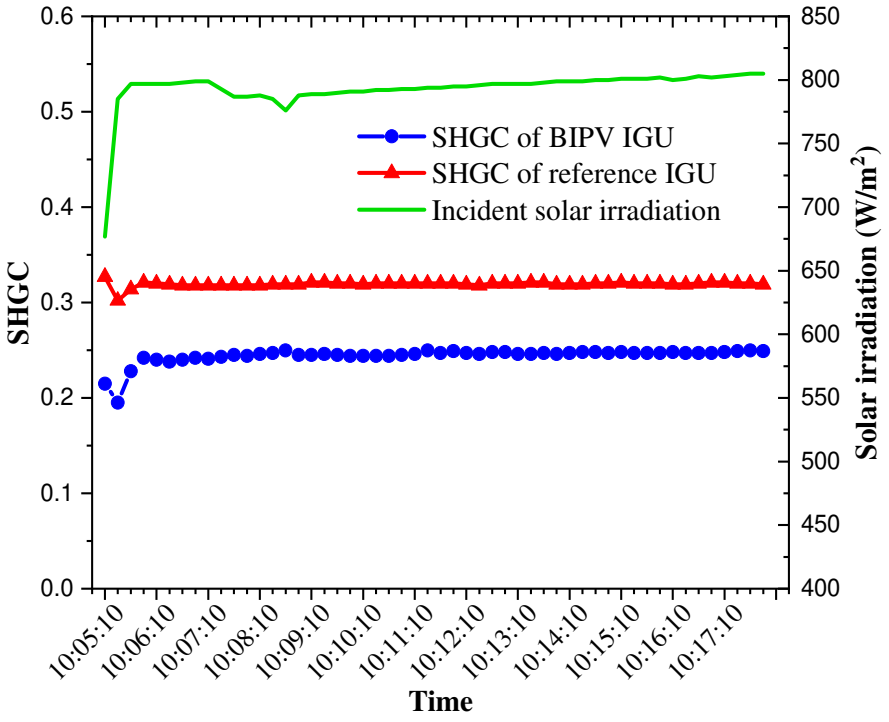

Figure 10 Comparison of SHGCs between BIPV IGU and reference IGU

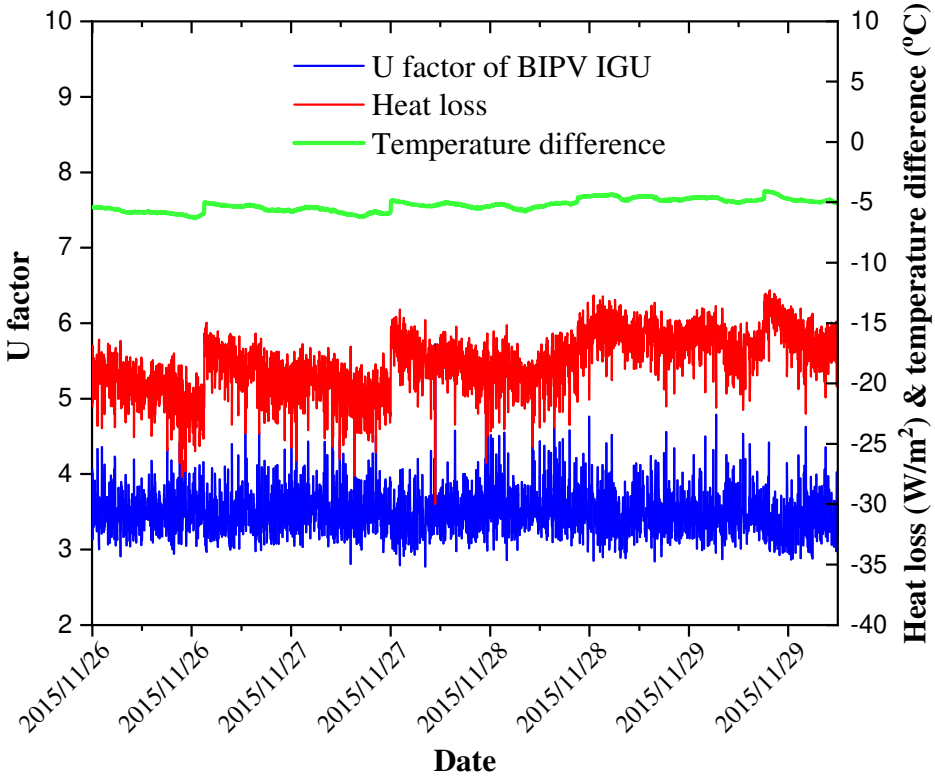

Figure 11 U-factor of the BIPV IGU (the average U-factor is 3.5) [43]

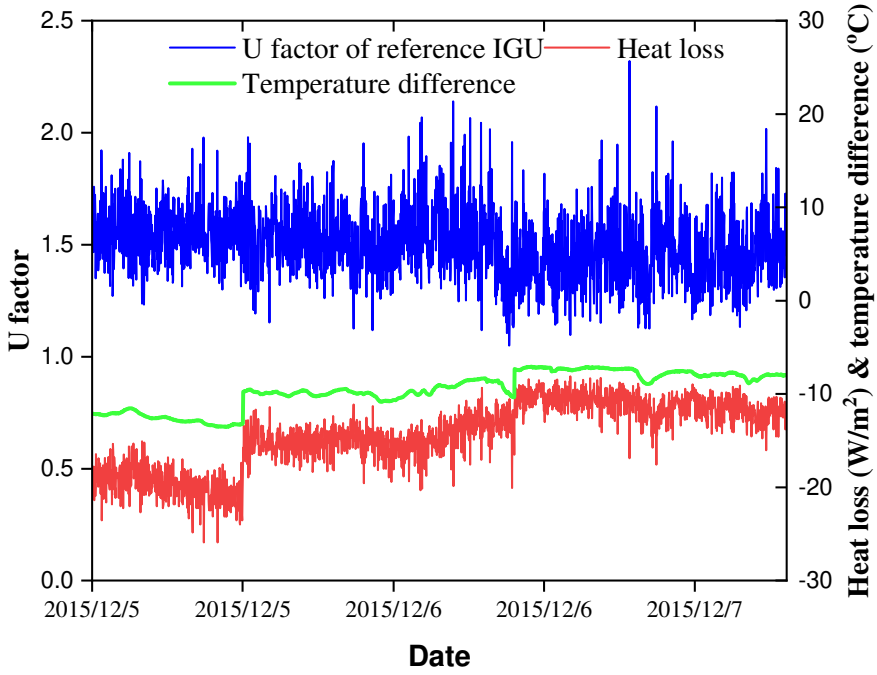

Figure 12 U-factor of the reference IGU (the average U-factor is 1.5)

4.2 HVAC electricity use

During the whole test period, various parameters related to HVAC electricity use in the both test cells (XRA and XRB) were measured and recorded. The measured parameters included water flow rates of heating and chilled water, supply and return water temperatures in heating and chilled water loops, air flow velocities in supply and return ductworks, supply and return air flow temperatures, as well as the real-time electricity consumption of water pumps and air handling units (AHUs). Based on the above data, the HVAC electricity uses in both XRA (where BIPV IGUs were installed) and XRB (where reference IGUs were installed) were calculated.

4.2.1 Results under the south orientation

From Oct. 20 to Oct. 23, 2015, both the BIPV IGU and the reference IGU were facing due south. The indoor air set point temperatures in both XRA and XRB were 17 ℃. Both the Venetian blinds behind the BIPV IGU and the reference IGU were pulled up. In this experimental case, a comparison of chilled water energy consumption in both XRA and XRB is presented in Figure 13. It is seen that the chilled water energy consumption in XRA was obviously less than that in XRB and the total chilled water energy consumptions in XRA and XRB were 95420 Wh and 121018 Wh, respectively. Therefore, the XRA test cell equipped with BIPV IGU reduced 21.1% chilled water energy consumption compared to the XRB during this period. Assuming the coefficient of performance (COPs) of chiller plants was 3.0, the electricity use of chiller plants for XRA and XRB was calculated. Finally, the HVAC electricity use in both XRA and XRB was

calculated by counting up the electricity uses of chiller plants, air handling units and water pumps, and the results are presented in Figure 14. The total HVAC electricity uses of XRA and XRB were 66075 Wh and 75822 Wh, respectively. Thus, the BIPV IGU reduced 12.9% HVAC electricity use compared to the reference IGU under the experimental conditions of the south orientation, 17 ℃ set point temperature and both Venetian blinds were pulled up.

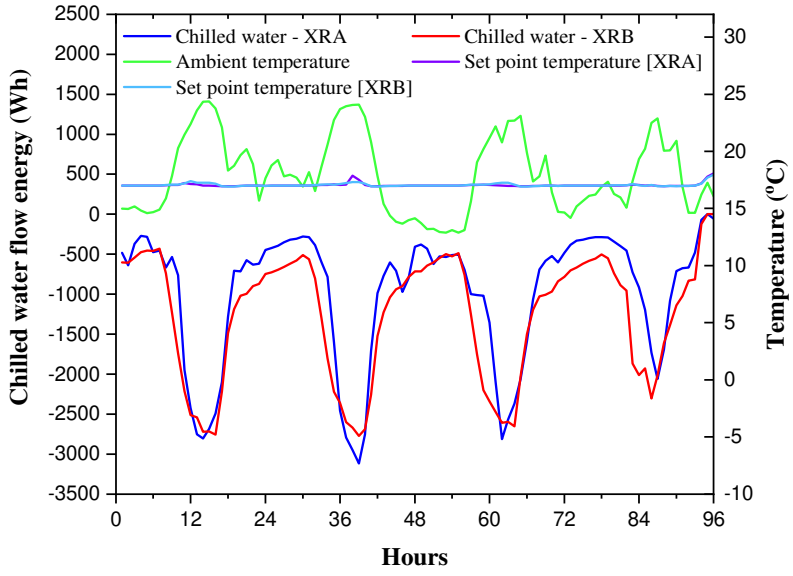

Figure 13 Comparison of chilled water energy consumption between XRA and XRB from Oct. 20 to Oct. 23, 2015

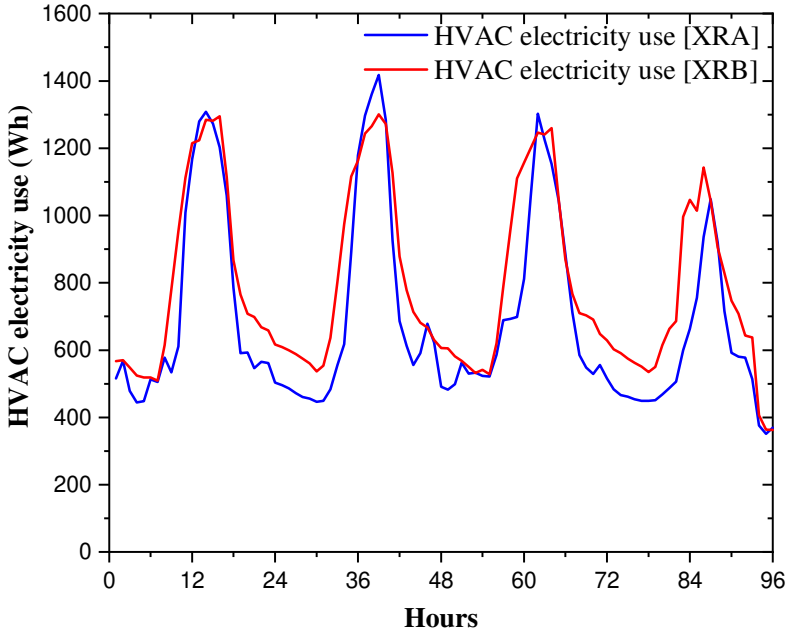

Figure 14 Comparison of HVAC electricity uses between XRA and XRB from Oct. 20 to Oct. 23, 2015

From Oct. 24 to Oct. 27, 2015, the indoor air set point temperatures in both XRA and XRB were adjusted to 18 ℃, while the other conditions were unchanged. In this experimental case, the chilled water energy consumption in XRA was also obviously less than that in XRB, as shown in Figure 15, and the total chilled water energy consumptions of XRA and XRB were 64749 Wh and 83598 Wh, respectively. The XRA test cell equipped with BIPV IGU reduced 22.5% chilled water energy consumption compared to XRB during this period. The HVAC electricity uses of XRA and XRB during this period are presented in Figure 16. The total HVAC electricity uses of XRA and XRB were 55648 Wh and 63103 Wh, respectively. Thus, the BIPV IGU reduced 11.8% HVAC electricity use compared to the reference IGU under the experimental conditions of THE south orientation; 18℃ set point temperature, and both Venetian blinds were pulled up.

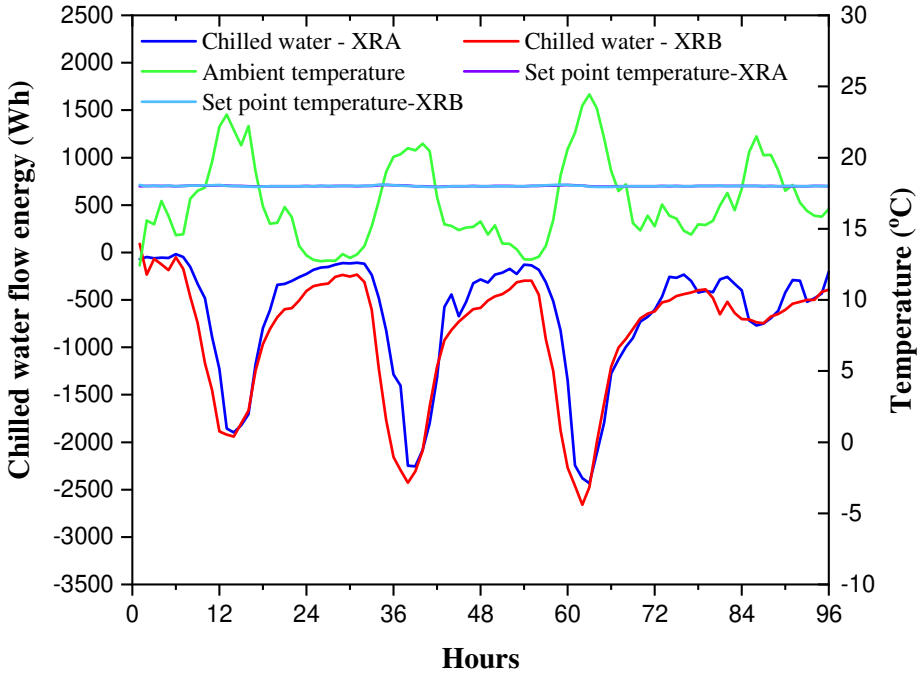

Figure 15 Comparison of chilled water energy consumption between XRA and XRB from Oct. 24 to Oct. 27, 2015

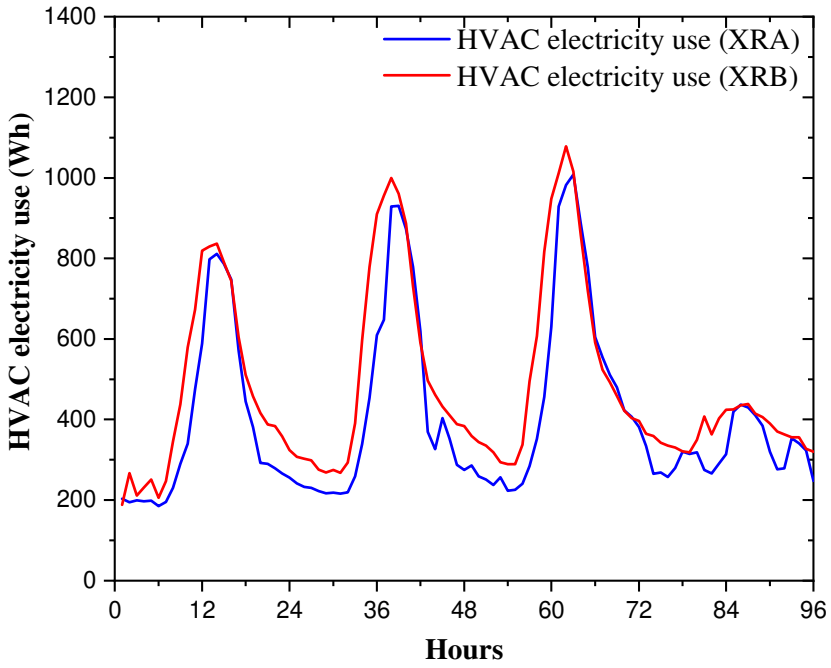

Figure 16 Comparison of HVAC electricity uses between XRA and XRB from Oct. 24 to Oct. 27, 2015

4.2.2 Results under the southeast orientation

From Nov. 01 to Nov. 06, 2015, the XR test bed was rotated to the southeast orientation, the set point temperature was kept at 18 ℃, and the both Venetian blinds in XRA and XRB were pulled down. The main purpose of rotating the test bed to different orientations was to measure and evaluate the overall energy performance (power, thermal and daylighting performance) of the BIPV IGU under different orientations such that to identify the optimum orientation regarding energy-efficient for installation.

In this case, the chilled water energy consumption in XRA was a little higher than that in XRB, as shown in Figure 17, and the total chilled water energy consumptions in XRA and XRB were 56996 Wh and 56562 Wh, respectively. The XRA test cell equipped with BIPV IGU consumed 0.8% more chilled water energy compared to the XRB during this period. Even though XRA had higher chilled water energy consumption than XRB, its HVAC electricity use was still lower than that of XRB, as shown in Figure 18, due to the less electricity uses for air handling units and water pumps. The total HVAC electricity uses in XRA and XRB were 70036 Wh and 71629 Wh, respectively. The BIPV IGU reduced only 2.2% HVAC electricity use compared to the reference IGU under the experimental conditions of the southeast orientation; 18℃ set point temperature and both Venetian blinds being pulled down. The above results showed that the BIPV IGU facing southeast orientation had much lower HVAC energy saving potential than facing south orientation. The reasons can be explained from two aspects. When the XR test bed rotated to TH southeast orientation, on the one hand, the west wall of the XRA test cell received more solar heat gain which resulted in a considerable increase of cooling load, on the other hand, as the XR

test bed was close to another test bed, a part of the reference IGUs was shaded by the adjacent test bed at morning, thus, the solar heat gain of the reference IGUs was obviously reduced in the southeast orientation.

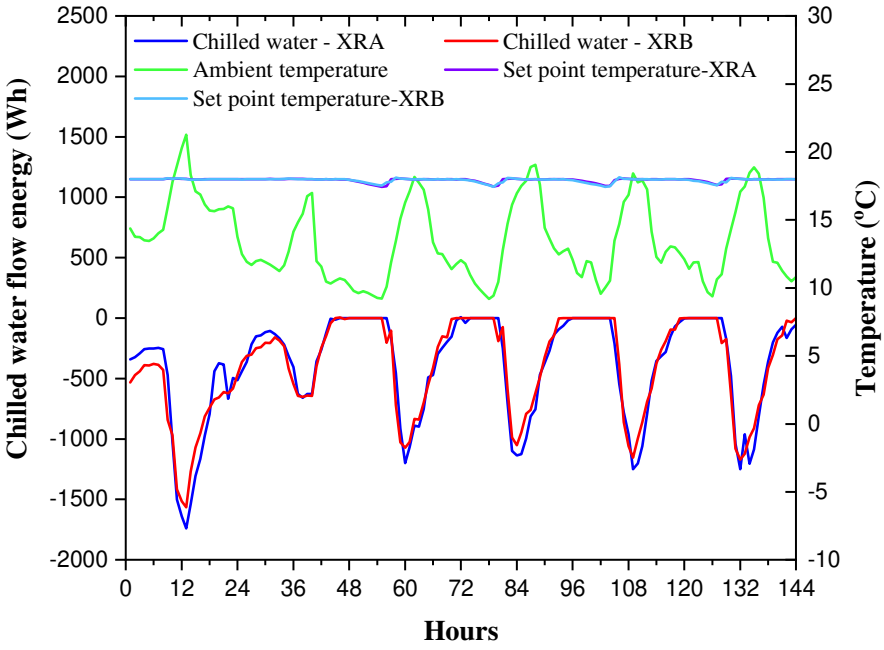

Figure 17 Comparison of chilled water energy consumption between XRA and XRB from Nov. 01 to Nov.06, 2015

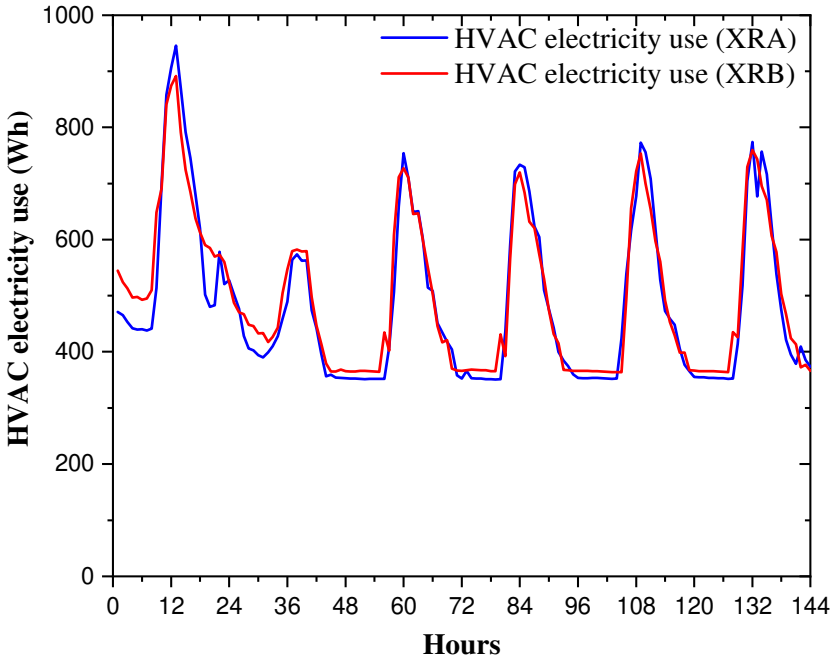

Figure 18 Comparison of HVAC electricity uses between XRA and XRB from Nov. 01 to Nov. 06, 2015

4.2.3 Results under the west orientation

From Dec. 05 to Dec. 08 2015, the test bed was rotated to the west orientation and the indoor air set point temperatures in both XRA and XRB were adjusted to 25 ℃ for heating. In this case, the hot water energy consumption in XRA was much higher than that in XRB due to its higher U-factor, as shown in Figure 19, and the total hot water energy consumptions in XRA and XRB were 99858 Wh and 67711 Wh, respectively. The XRA test cell equipped with BIPV IGU consumed 47.5% more hot water energy compared to the XRB during this period. Compared to XRB, XRA consumed much more HVAC electricity use for space heating, as shown in Figure 20. The total HVAC electricity uses of XRA and XRB were 62180 Wh and 52136 Wh, respectively. The BIPV IGU consumed 19.3% more HVAC electricity compared to the reference IGU under the experimental conditions of west orientation, 25℃ set point temperature with both Venetian blinds being pulled up. The test results indicated that the Low-E coating deposited on the surface facing to indoor room achieved much better thermal insulation performance than that facing to outside. Thus, the Low-E coating should be placed on the fourth surface of the BIPV IGU in future design to improve its thermal insulation performance.

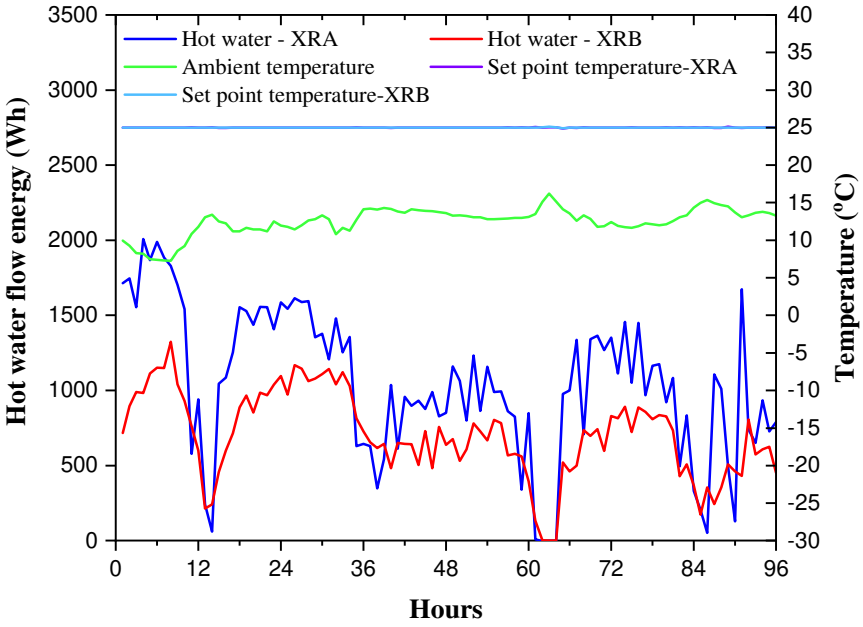

Figure 19 Comparison of hot water energy consumption between XRA and XRB from Dec. 05 to Dec.08, 2015

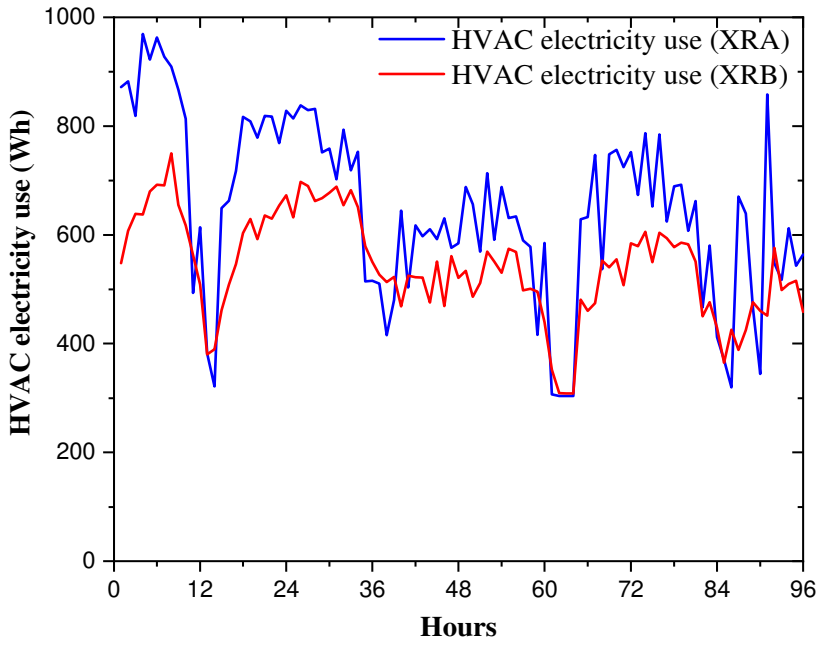

Figure 20 Comparison of HVAC electricity uses between XRA and XRB from Dec. 05 to Dec.08, 2015

To have a complete understanding of the HVAC energy saving potential of the BIPV IGU, an overview of energy conservation results under different orientations, different set point temperatures and different shade positions are listed in Table 4. In general, the BIPV IGU had much higher energy saving potential in the south orientation than in southeast orientation. The average HVAC electricity saving was 11.6% for the south facing orientation, but it was only 2.6% for the southeast facing orientation. Eliminating the two influence factors mentioned before, an energy saving potential of 8-10% might be expected for the southeast orientation. Due to high U-factor, the thermal insulation performance of the BIPV IGU was worse than that of the reference IGU. For space heating, the XRA test cell equipped with BIPV IGUs consumed 19.3% more HVAC electricity than the XRB test cell installed with reference IGUs. Also, the shade position also affected the HVAC electricity saving of the BIPV IGU. The BIPV IGU had higher energy saving potential in the case of both Venetian blinds being pulled up, followed by blinds in XRA being pulled up but being pulled down in XRB, and the worst case was both blinds being pulled down.

Table 4 Overview of energy saving results of the BIPV IGU under different conditions [44]

Test periods	Orientation	Set point temp.	Blinds position	Chilled (Heating) water energy (Wh)	HVAC electricity use (Wh)	Energy saving of BIPV IGU
10/01-10/06	South	21℃	Both down	XRA:73295 XRB:78857	XRA:98807 XRB:105184	6.1%
10/20-10/23	South	17℃	Both up	XRA:95420	XRA:66075	12.9%

				XRB:121018	XRB:75822	
10/24-10/27	South	18℃	Both up	XRA:64749	XRA:55648	11.8%
				XRB:83598	XRB:63103	
10/28-10/30	Southeast	18℃	Both up	XRA:57166	XRA:44929	3.0%
				XRB:59794	XRB:46318	
11/01-11/06	Southeast	18℃	Both down	XRA:56996	XRA:70036	2.2%
				XRB:56562	XRB:71629	
11/18-11/22	South	18℃	Both up	XRA:60988	XRA:62942	18%
				XRB:98111	XRB:76734	
12/05-12/08	West	25℃	Both up	XRA:99858	XRA:62180	-19.3%
		(heat)		XRB:67711	XRB:52136	

4.3 Power Generation Performance

Compared to other advanced window technologies, BIPV windows are distinguished by the ability to transform a portion of the incident solar irradiation into useful electrical power through the photovoltaic effect. During this test, the incident solar irradiation and the real-time electricity power output were measured, the energy conversion efficiency of the BIPV IGU was also calculated based on the measured data. Figure 21 presents the daily electricity output and energy conversion efficiency in October 2015. It is seen that the highest daily electricity output was 2.54 kWh (equal to 0.28 kWh/m^2), occurred on Oct.21, 2015 when the BIPV IGU was facing south orientation. The daily energy conversion efficiency of the active solar cell area (3 m^2) was more or less 15% on sunny days, but it was much lower on overcast days because it is well known that crystalline silicon solar cells have lower efficiency under low solar irradiation level. Moreover, the daily average electricity outputs under different orientations were calculated. They were 1.58 kWh (0.18 kWh/m^2), 1.94 kWh (0.22 kWh/m^2) and 1.91 kWh (0.21 kWh/m^2) for the southeast, south and southwest orientations, respectively. The BIPV IGU generated almost the same daily average electricity in south and southwest orientations, which is higher than that of southeast orientation by 19%. Thus, a conclusion can be drawn that south and southwest orientations are more suitable for installing BIPV IGU regarding increasing power generation.

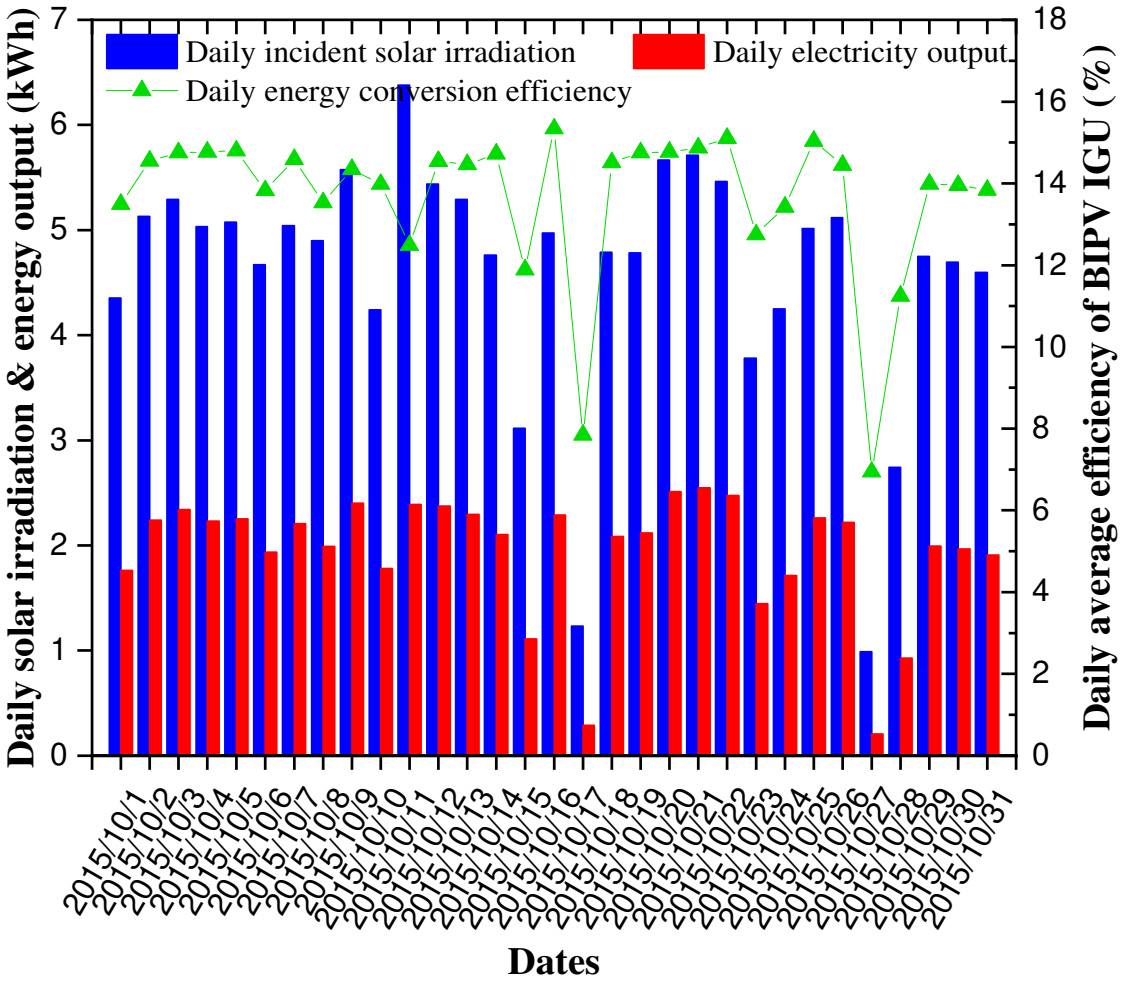

Figure 21 Daily electricity output and energy conversion efficiency in Oct. 2015

4.4 Daylighting performance

The objective of daylighting measurement and analysis is to evaluate the trade-offs associated with the BIPV IGU between daylight, glare, and lighting energy use. High dynamic range (HDR) cameras and photometers were employed to measure the luminance at seated eye height parallel to and facing the window, as well as the workplane illuminance, respectively. Figure 22 illustrates the layout and location of sensors in the both test cells. During the test, the Venetian blinds were either fully raised or fully lowered with a slat angle that just blocked direct sunlight. The electric lighting was set to a fixed lighting level of 300 lux, providing a stable ambient lighting level so that visual discomfort could be evaluated with an adequate baseline for visual adaptation.

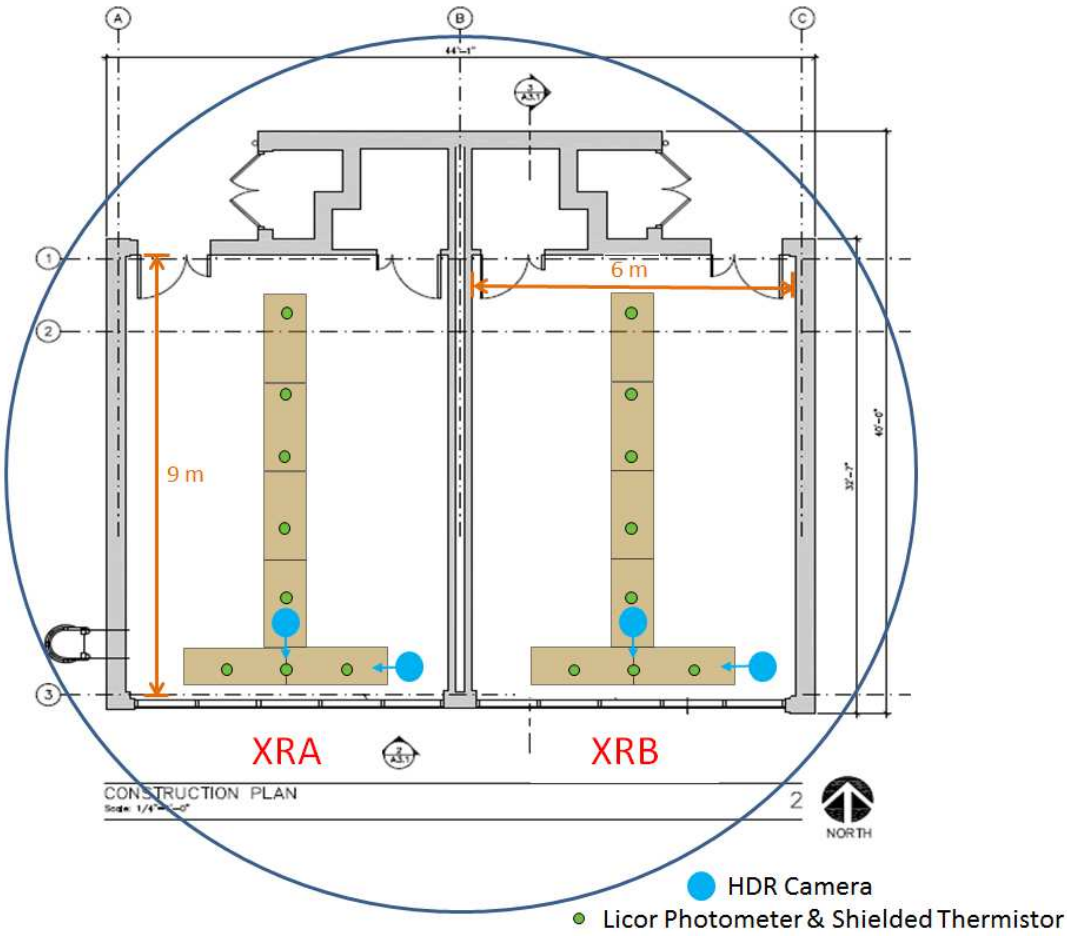

Figure 22 Location of sensors in the BIPV and reference test cells

4.4.1 Visual comfort

Hemispherical field-of-view luminance measurements were made at two sites of each test cell at seated eye height 1.2 m above the floor parallel to and facing the window, as shown in Figures 22 and 23. These locations represent a conservative, worst-case evaluation of discomfort glare from the window. Measurements were made using commercial-grade digital cameras (Canon 60D) equipped with an equidistant fisheye lens (Sigma E 4.5 mm f/2.8). Bracketed low dynamic range (LDR) images were taken automatically at 10-min intervals then converted into a calibrated high dynamic range (HDR) image, which was then used to assess discomfort glare.

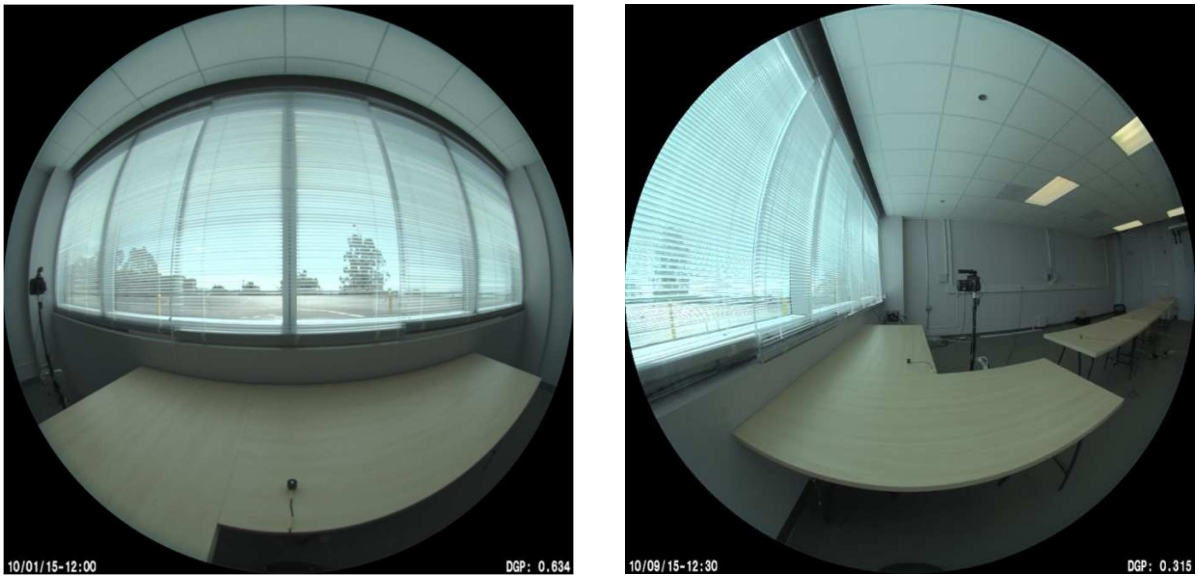

(a) **(b)**

Figure 23 (a) Fisheye view from seated height looking toward the window at 1 m from the window; (b) fisheye view from seated height looking parallel to the window at 1 m from the window.

The Daylight Glare Probability (DGP) index was used to evaluate discomfort glare of the BIPV IGU and the reference IGU. This index was derived from a comprehensive statistical analysis of HDR data and subjective response in a full-scale private office testbed that was retrofit with a variety of daylighting measures [45]. The 10-min interval DGP values were used to calculate summary values for the day from 8 AM to 6 PM local time, which were then compared to the four classified levels of glare tolerance as shown in Table 5. Subjective ratings of just imperceptible, just perceptible, just disturbing, and just intolerable glare correspond to DGP values of 0.30, 0.35, 0.40, and 0.45, respectively.

Table 5 Daylight Glare Probability (DGP) classification

Max DGP of 95% office time	and	Average DGP of 5% office time	Class	Meaning
≤0.35 ("imperceptible" glare)	and	≤ 0.38 ("perceptible" glare)	A	Best
	and	> 0.38	B	Good
≤ 0.40 ("perceptible" glare)	and	≤ 0.42 ("disturbing" glare)	B	Good
	and	> 0.42	C	Reasonable
≤ 0.45 ("disturbing" glare)	and	≤ 0.53 ("intolerable" glare)	C	Reasonable
	and	> 0.53	Discomfort	Discomfort
> 0.45 ("intolerable" glare)			Discomfort	Discomfort

The DGP levels at a seated view facing the BIPV IGU and the reference IGU are shown in Table 6 in Appendix A. The results indicated that for the seated view looking toward the IGUs, discomfort glare from the IGU was inadequately controlled over the entire period irrespective of reference or BIPV condition, window orientation and whether the blinds were raised or lowered. However, discomfort glare was lower with the BIPV IGU compared to the reference IGU due to the combined effect of both the visible transmittance of the transparent glass and the lower percentage of transparent window area. The "C" class of DGP occurred on a few days in the XRA cell (equipped with BIPV IGU), but occurred only one day in the XRB cell. In summary, a lower transmittance BIPV IGU will be needed to bring overall discomfort levels to below the "just perceptible" glare level of 0.35, if the most conservative viewpoint near the window is used for the assessment. Thus, a study on daylighting performance and visual comfort under different transmittances is recommended to be conducted in future to identify the optimal transmittance which can not only achieve the acceptable visual comfort and daylight performance but also maximize the overall energy performance of BIPV IGU.

4.4.2 Lighting energy

Although the BIPV IGU reduced glare compared to the reference IGU due to its lower transmittance, it was also expected to result in increased lighting energy use and less indoor brightness. In each test cell, the lighting energy use due to daylight dimming was determined based on measured illuminance levels at the workplane and the dimming profile of LED and fluorescent fixtures, which were derived from a parallel on-site study. The LED installed lighting power density (LPD) was 0.51 W/ft^2. Assuming the dimming profile from full power was linear, 64.9 W was required for LED to produce 300 lux at the workplane in each 3 m deep zone. The T5 fluorescent system had an installed LPD of 0.59 W/ft^2, with 123.6 W required to produce 300 lux in each 3 m zone. Sensors at a distance of 2.5 m, 5.5 m and 8.5 m from the window were used to determine daily lighting energy use between 8 AM and 6 PM local time and the results are listed in Table 7 in Appendix A. It is seen that the lighting energy use in XRB with reference IGU is almost always lower than that in XRA with BIPV IGU irrespective of using LED or fluorescent fixtures. On clear days, the average lighting energy use in XRA and XRB were 733 and 380 Wh/day respectively for fluorescent fixtures used, and were 352 and 182 Wh/day respectively for LED fixtures used. Compared to fluorescent lighting, LED lighting fixture saved about half of lighting energy use in both XRA and XRB test cells. In summary, daily lighting energy use was increased for the BIPV with blinds case by 188 Wh/day (77.4%) or 337 Wh/day (61.4%) on average compared to the reference IGU with blinds if dimmable LED or fluorescent lighting was used over the 9 m deep space, respectively. However, it is worth noting that if glare is reduced further by using lower transmittance glazing or a closed slat angle, lighting energy use will increase in both test cells, but the magnitude of the increase will be very low.

4.5 Overall energy saving potential

To have a complete understanding of the overall energy saving potential of the BIPV IGU, an overview of energy consumption and power generation results of the both test cells are listed in Table 8 in Appendix A. Assuming that LED lighting will be prevalent in the new building stock for the next decade, the lighting electricity use of the XRA cell with BIPV IGU is higher than that of XRB cell, but the increment was relatively small compared to the amount of power generation of the BIPV IGU. Also, the BIPV IGU could also reduce about 10% electricity use for cooling due to its lower SHGC. For XRA test cell, the increase in lighting energy use is about 166 Wh/day, while the average BIPV generation for the same period is 1985 Wh/day and the energy saving in HVAC electricity use is 1533 Wh/day. The net energy saving is therefore 3352 Wh/day. On average, the XRA cell with BIPV IGU saved 16.8% electricity use compared to the XRB cell with reference IGU under the south orientation. It is a quite impressive achievement for a single energy saving technique, which could reduce the whole room's electricity use by one-sixth.

At present, the cost of the solar cell material is very low, and the price of crystalline solar cell itself is usually lower than 0.15 dollar per watt. However, the cost of BIPV IGU is relatively high due to the additional machine need of the production process. With the large-scale production and the improvement of the process, it is believed that the cost will fall sharply and there will be a good profit for BIPV IGU.

5. Conclusions

A side by side comparative study between a novel BIPV insulated glass unit (IGU) and a Low-E coated reference IGU was conducted on the Facility for Low Energy Experiment in Buildings (FLEXLAB) to fully identify the overall energy performance and energy saving potential of the BIPV IGU under real world conditions.

Compared to reference IGU, the BIPV IGU had lower solar heat gain coefficient (SHGC) due to its lower solar transmittance but has higher U-factor because the Low-E coating was not placed on an appropriate surface. To further improve the thermal insulation performance of this kind of BIPV IGU, the Low-E coating is recommended to be deposited on the fourth surface with facing to the cavity.

The HVAC electricity saving potential of the BIPV IGU relative to the reference IGU under different orientations, different set point temperatures and different shade positions were determined via comparative experiment. The average HVAC electricity saving was 11.6% for the south facing BIPV IGU, but it was only 2.6% for the southeast facing one during the test period. However, if the two influence factors for the southeast facing case are eliminated, an HVAC electricity saving potential of 8-10% might be expected. The BIPV IGU had worse

thermal insulation performance than the reference IGU due to its high U-factor, which directly resulted in a 19.3% more HVAC electricity use for space heating for the test cell with BIPV IGU.

Distinguished from the reference IGU, the BIPV IGU generated electricity on the site of buildings through the photovoltaic effect. The highest daily electricity output was 0.28 kWh/m^2 when the BIPV IGU was facing south orientation during the test period. For different orientations, the daily average electricity outputs were 0.18, 0.22 and 0.21 kWh/m^2 for the southeast, south and southwest, respectively. Based on the experimental data, a conclusion was drawn that south and southwest orientations are more suitable for installing BIPV IGU regarding increasing power generation.

Daylighting measurement and analysis were carried out to evaluate the trade-offs associated with the BIPV IGU between daylight, glare, and lighting energy use. The results indicated that discomfort glare from IGUs was inadequately controlled in the both test cells. However, discomfort glare was lower with the BIPV IGU compared to the reference IGU due to the combined effect of both the visible transmittance of the transparent glass and the lower percentage of transparent window area. If the most conservative viewpoint near the window is used for the assessment, a lower transmittance BIPV IGU will be needed to bring overall discomfort levels in the test cell to below the "just perceptible" glare level of 0.35. Thus, a study on daylighting performance and visual comfort under different transmittances is recommended to be conducted in future to identify the optimal transmittance which can not only achieve the acceptable visual comfort and daylight performance but also maximize the overall energy performance of BIPV IGU.

The net energy saving potential associated with the novel BIPV IGU was identified based on the power, thermal and daylighting performance during the test period. For the XRA test cell with BIPV IGU, the increase in lighting energy use was about 166 Wh/day, while the average BIPV generation was 1985 Wh/day and the energy saving in HVAC electricity use was 1533 Wh/day. The net energy saving was therefore 3352 Wh/day for the BIPV IGU studied. On average, the XRA cell with BIPV IGU saved 16.8% electricity use compared to the XRB cell with reference IGU under the south orientation. It is really a quite impressive achievement. Further studies and improvement on the energy conversion efficiency of solar cells, the optimal transmittance as well as the thermal insulation properties would make this technology more energy-efficient and affordable. It is worth noted that the above energy performance data was only derived from two months' experimental results. Thus, it might not represent the performance for a year. In future, we will focus on developing a numerical model to simulate the annual overall energy performance of the BIPV IGU under different climate zones.

Acknowledgements

This work was supported by the Assistant Secretary for Energy Efficiency and Renewable Energy, Building Technologies Program, of the U.S. Department of Energy under Contract no. DE-AC02-

05CH11231. We also appreciate technical supports and useful discussions with Mr. Udi Paret and Mr. Nadeem Haque from Solaria Co.

Appendix A. Tables

Table 6 Daylight glare probability (DGP) levels for a seated view looking normal to the IGUs

Date	Light	Blinds		Sky condition	Camera-facing window					
		XRA	XRB		XRA-BIPV			XRB-Reference		
					Mean 5%	Max 95%	Class	Mean 5%	Max 95%	Class
10/1	off	down	down	dyn+clear	0.460	0.437	C	0.738	0.653	discomfort
10/2	off	down	down	clear	0.425	0.424	C	0.624	0.623	discomfort
10/3	off	down	down	clear	0.437	0.436	C	0.648	0.646	discomfort
10/4	off	down	down	clear	0.434	0.432	C	0.642	0.640	discomfort
10/5	off	down	down	clear	0.437	0.435	C	0.648	0.645	discomfort
10/6	off	down	down	clear	0.685	0.437	discomfort	0.834	0.832	discomfort
10/7	off	down	down	clear	0.447	0.444	C	0.686	0.676	discomfort
10/8	on	down	down	dynamic	0.464	0.459	discomfort	0.718	0.708	discomfort
10/9	on	down	down	clear	0.438	0.437	C	0.654	0.653	discomfort
10/10	on	down	down	clear	0.474	0.446	C	0.721	0.675	discomfort
10/11	on	down	down	clear	0.444	0.443	C	0.666	0.665	discomfort
10/12	on	down	down	clear	0.441	0.439	C	0.659	0.658	discomfort
10/13	on	down	down	clear	0.452	0.451	discomfort	0.688	0.686	discomfort
10/14	on	down	down	clear	0.498	0.489	discomfort	0.796	0.772	discomfort

10/15	on	up	down	dynamic	0.872	0.869	discomfort	0.785	0.717	discomfort
10/16	on	up	down	clear	0.872	0.871	discomfort	0.747	0.736	discomfort
10/17	on	up	down	overcast	0.542	0.459	discomfort	0.420	0.399	C
10/18	on	up	down	dynamic	0.877	0.874	discomfort	0.821	0.798	discomfort
10/19	on	up	down	dyn+clear	0.881	0.878	discomfort	0.771	0.753	discomfort
10/20	on	up	up	clear	0.873	0.872	discomfort	0.846	0.844	discomfort
10/21	on	up	up	clear	0.873	0.872	discomfort	0.844	0.842	discomfort
10/22	on	up	up	clear	0.874	0.872	discomfort	0.842	0.841	discomfort
10/23	on	up	up	dynamic	0.875	0.873	discomfort	0.853	0.851	discomfort
10/24	on	up	up	dynamic	0.876	0.872	discomfort	0.846	0.845	discomfort
10/25	on	up	up	clear	0.875	0.873	discomfort	0.848	0.843	discomfort
10/26	on	up	up	clear	0.878	0.876	discomfort	0.863	0.857	discomfort
10/27	on	up	up	cloudy	0.478	0.405	C	0.654	0.614	discomfort

Table 7 Daily lighting energy use (Wh) and percentage savings

Date	Light	Blinds		Sky condition	Fluorescent lighting energy use (Wh)			LED lighting energy use (Wh)		
		XRA	XRB		XRA BIPV	XRB ref.	Savings	XRA BIPV	XRB ref.	Savings
10/3	off	down	down	clear	952	418	-128%	453	198	-129%
10/4	off	down	down	clear	977	436	-124%	466	206	-126%
10/5	off	down	down	clear	955	428	-123%	455	202	-126%

10/6	off	down	down	clear	934	497	-88%	453	233	-94%
10/7	off	down	down	clear	909	395	-130%	432	187	-131%
10/8	on	down	down	dynamic	1041	508	-105%	501	239	-110%
10/9	on	down	down	clear	999	430	-132%	477	205	-132%
10/10	on	down	down	clear	1527	1005	-52%	760	505	-51%
10/11	on	down	down	clear	970	436	-122%	461	208	-122%
10/12	on	down	down	clear	966	433	-123%	460	206	-123%
10/13	on	down	down	clear	879	395	-123%	411	187	-120%
10/14	on	down	down	clear	849	354	-140%	405	169	-139%
10/15	on	up	down	dynamic	1105	1137	3%	547	565	3%
10/16	on	up	down	clear	479	429	-12%	234	209	-12%
10/17	on	up	down	overcast	1835	2010	9%	917	1003	9%
10/18	on	up	down	dynamic	583	607	4%	285	296	4%
10/19	on	up	down	dyn+clear	588	638	8%	294	312	6%
10/20	on	up	up	clear	395	125	-216%	191	58	-229%
10/21	on	up	up	clear	432	126	-242%	208	59	-250%
10/22	on	up	up	clear	354	130	-172%	169	61	-175%
10/23	on	up	up	dynamic	787	430	-83%	384	204	-88%
10/24	on	up	up	dynamic	571	280	-104%	275	136	-103%
10/25	on	up	up	clear	587	359	-64%	291	176	-65%

10/26	on	up	up	clear	497	256	-94%	241	123	-96%
10/27	on	up	up	cloudy	1978	1455	-36%	997	122	-38%

Table 8 Comparison of electricity uses between cell A and cell B under the south orientation [44]

	XRA (BIPV IGU)				XRB (Reference IGU)			Energy saving	
Dates	HVAC electricity use (kWh)	Lighting electricity use (LED) (kWh)	BIPV IGU Power generation (kWh)	Net electricity use (kWh)	HVAC electricity use (kWh)	Lighting electricity use (LED) (kWh)	Net electricity use (kWh)	Total energy saving in XRA (kWh)	Energy saving in XRA (%)
10/1/2015	16.14	1.75	1.76	16.13	17.40	1.57	18.97	2.85	15.00
10/2/2015	17.36	0.43	2.24	15.55	18.04	0.21	18.25	2.70	14.78
10/3/2015	15.76	0.45	2.34	13.87	16.92	0.20	17.11	3.24	18.95
10/4/2015	15.79	0.47	2.23	14.02	16.73	0.21	16.94	2.92	17.23
10/5/2015	17.10	0.46	2.25	15.31	18.13	0.20	18.33	3.02	16.50
10/6/2015	16.65	0.45	1.94	15.17	17.97	0.23	18.20	3.03	16.64
10/7/2015	25.85	0.43	2.21	24.08	27.85	0.19	28.04	3.96	14.14
10/8/2015	29.61	0.50	1.99	28.13	31.04	0.24	31.28	3.15	10.08
10/9/2015	31.25	0.48	2.40	29.32	29.83	0.21	30.03	0.71	2.35
10/10/2015	29.11	0.76	1.78	28.09	28.78	0.50	29.29	1.20	4.09
10/11/2015	28.16	0.46	2.39	26.23	29.08	0.21	29.29	3.06	10.46
10/12/2015	29.18	0.46	2.37	27.27	30.66	0.21	30.87	3.59	11.64
10/13/2015	25.57	0.41	2.30	23.68	29.09	0.19	29.28	5.59	19.11
10/14/2015	21.09	0.40	2.10	19.39	23.35	0.17	23.52	4.12	17.53
10/15/2015	18.38	0.55	1.11	17.82	18.55	0.56	19.11	1.29	6.77
10/16/2015	18.85	0.23	2.29	16.80	19.88	0.21	20.09	3.29	16.37
10/17/2015	13.03	0.92	0.29	13.66	15.54	1.00	16.54	2.88	17.40
10/18/2015	13.37	0.28	2.09	11.57	15.62	0.30	15.91	4.34	27.29
10/19/2015	16.04	0.29	2.12	14.22	18.05	0.31	18.37	4.15	22.59
10/20/2015	17.64	0.19	2.51	15.32	19.61	0.06	19.67	4.35	22.11
10/21/2015	17.51	0.21	2.55	15.17	19.88	0.06	19.94	4.76	23.89
10/22/2015	17.25	0.17	2.48	14.94	19.55	0.06	19.62	4.68	23.83
10/23/2015	13.68	0.38	1.45	12.61	16.78	0.20	16.98	4.37	25.72
10/24/2015	13.43	0.28	1.71	11.99	15.35	0.14	15.49	3.50	22.59
10/25/2015	14.47	0.29	2.26	12.49	16.94	0.18	17.12	4.62	27.01
10/26/2015	15.85	0.24	2.22	13.87	17.67	0.12	17.79	3.92	22.04
10/27/2015	11.91	1.00	0.21	12.70	13.14	0.72	13.86	1.16	8.40

References

[1] Buildings Energy Data Book: 1.1 Buildings Sector Energy Consumption. Energy Efficiency & Renewable Energy. Department of Energy, the United States, March 2012.

[2] Arasteh D, Selkowitz S, Apte J. Zero Energy Windows. Proceedings of the 2006 ACEEE Summer Study on Energy Efficiency in Buildings, August 13-18, 2006, Pacific Grove, CA. <http://gaia.lbl.gov/btech/papers/60049.pdf>

[3] Kamal A.R. Ismail, Carlos T. Salinas, Jorge R. Henriquez. Comparison between PCM filled glass windows and absorbing gas filled windows. Energy and Buildings 2008; 40(5):710–719.

[4] Collins RE and Simko TM. Current status of the science and technology of vacuum glazing. Solar Energy 1998; 62(3): 189–213.

[5] Chow TT, Li CY, Lin Z. Innovative solar windows for cooling-demand climate. Solar Energy Materials and Solar Cells 2010; 94(2): 212–220.

[6] Aydın O. Conjugate heat transfer analysis of double pane windows. Building and Environment 2006; 41(2): 109–116.

[7] Kaklauskas A, Zavadskas EK, Raslanas S, Ginevicius R, Komka A, Malinauskas P. Selection of Low-E windows in retrofit of public buildings by applying multiple criteria method COPRAS: A Lithuanian case. Energy and Buildings 2006; 38 (5):454–462.

[8] Papaefthimiou S, Syrrakou E, Yianoulis P. Energy performance assessment of an electrochromic window. Thin Solid Films 2006; 502: 257–264.

[9] Peng JQ, Curcija DC, Lu L, Selkowitz SE, Yang HX, Mitchell R. Developing a method and simulation model for evaluating the overall energy performance of a ventilated semi-transparent photovoltaic double-skin façade. Prog. Photovolt: Res. Appl. (2015).

[10] Fung YY, Yang HX. Study on thermal performance of semi-transparent building-integrated photovoltaic glazings. Energy Build 2008;40:341–50.

[11] Han J, Lu L, Yang HX. Thermal behavior of a novel type see-through glazing system with integrated PV cells. Build Environ 2009;44:2129–36.

[12] Han J, Lu L, Yang HX. Numerical evaluation of the mixed convective heat transfer in a double-pane window integrated with see-through a-Si PV cells with Low-E coatings. Appl Energy 2010;87:3431–7.

[13] Pal SK, Alanne K, Jokisalo J, Siren K. Energy performance and economic viability of advanced window technologies for a new Finnish townhouse concept. Appl Energy 2016;162:11–20.

[14] Chow T-T, Qiu Z, Li C. Potential application of ‘‘see-through” solar cells in ventilated glazing in Hong Kong. Sol Energy Mater Sol Cells 2009;93(2):230–8.

[15] He W, Zhang YX, Sun W, Hou JX, Jiang QY, Ji J. Experimental and numerical investigation on the performance of amorphous silicon photovoltaics window in East China. Build Environ 2011;46(2):363–9.

[16] Yoon JH, Shim SR, An YS, Lee KH. An experimental study on the annual surface temperature characteristics of amorphous silicon BIPV window. Energy and Buildings 2013; 62: 166–175.

[17] Chen FZ, Wittkopf SK, Ng PK, Du H. Solar heat gain coefficient measurement of semi-transparent photovoltaic modules with indoor calorimetric hot box and solar simulator. Energy and Buildings 2012;53:74–84.

[18] Lu L, Law KM. Overall energy performance of semi-transparent single-glazed photovoltaic (PV) window for a typical office in Hong Kong. Renew Energy 2013;49:250–4.

[19] Miyazaki T, Akisawa A, Kashiwagi T. Energy savings of office buildings by the use of semi-transparent solar cells for windows. Renew Energy 2005;30:281–304.

[20] Wong PW, Shimoda Y, Nonaka M, Inoue M, Mizuno M. Semi-transparent PV: thermal performance, power generation, daylight modelling and energy saving potential in a residential application. Renew Energy 2008;33:1024–36.

[21] Peng J, Lu L, Yang H, Han J. Investigation on the annual thermal performance of a photovoltaic wall mounted on a multi-layer façade. Appl Energy 2013;112:646–56.

[22] Cuce E, Young CH, Riffat SB. Thermal performance investigation of heat insulation solar glass: a comparative experimental study. Energy Build 2015;86:595–600.
[23] Motuziene V, Bielskus J. Assessment of overall performance of building integrated photovoltaics. In: The 9th International conference on environmental engineering. 22–23 May 2014, Vilnius (Lithuania); 2014.
[24] Bizzarri G, Gillott M, Belpoliti V. The potential of semitransparent photovoltaic devices for architectural integration: the development of device performance and improvement of the indoor environmental quality and comfort through case-study application. Sustainable Cities and Society 2011; 1: 178–185.
[25] Polo Lopez CS, Sangiorgi M. Comparison assessment of BIPV façade semi-transparent modules: further insights on human comfort conditions. International Conference on Solar Heating and Cooling for Buildings and Industry, 2013, Freiburg, Germany. Energy Procedia 2014; 48: 1419–1428.
[26] Ng PK, Mithraratne N. Lifetime performance of semi-transparent building integrated photovoltaic (BIPV) glazing systems in the tropics. Renew Sustain Energy Rev 2014;31:736–45.
[27] Lynn N, Mohanty L, Wittkopf S. Color rendering properties of semi-transparent thin-film PV modules. Build Environ 2012;54:148–58.
[28] Li DHW, Lam TNT, Cheung KL. Energy and cost studies of semi-transparent photovoltaic skylight. Energy Convers Manage 2009;50(8):1981–90.
[29] Chow TT, Fong KF, He W, Lin Z, Chan aLS. Performance evaluation of a PV ventilated window applying to office building of Hong Kong. Energy Build 2007;39(6):643–50.
[30] Leite Didoné E, Wagner A. Semi-transparent PV windows: a study for office buildings in Brazil. Energy Build 2013;67:136–42.
[31] Chae YT, Kim J, Park H, Shin B. Building energy performance evaluation of building integrated photovoltaic (BIPV) window with semi-transparent solar cells. Appl Energy 2014;129:217–27.
[32] Kapsis K, Athienitis AK. A study of the potential benefits of semi-transparent photovoltaics in commercial buildings. Sol Energy 2015;115:120–32.
[33] Park KE, Kang GH, Kim HI, Yu GJ, Kim JT. Analysis of thermal and electrical performance of semi-transparent photovoltaic (PV) module. Energy 2010;35:2681–7.
[34] Li DHW, Lam TNT, Chan WWH, Mak AHL. Energy and cost analysis of semi-transparent photovoltaic in office buildings. Appl Energy 2009;86(5):722–9.
[35]Xu S, Liao W, Huang J, Kang J. Optimal PV cell coverage ratio for semi-transparent photovoltaics on office building facades in central China. Energy and Buildings 2014; 77: 130–138.
[36] Olivieri L, Caamano-Martín E, Moralejo-Vazquez FJ, Martin-Chivelet N, Olivieri F, Neila-Gonzalez FJ. Energy saving potential of semi-transparent photovoltaic elements for building integration. Energy 2014; 76:572–583.
[37] Ng PK, Mithraratne N, Kua HW. Energy analysis of semi-transparent BIPV in Singapore buildings. Energy Build 2013;66:274–81.
[38] Jinqing Peng, Dragan C. Curcija, Lin Lu, Stephen E. Selkowitz, Hongxing Yang, Weilong Zhang. Numerical investigation of the energy saving potential of a semi-transparent photovoltaic double-skin facade in a cool-summer Mediterranean climate. Applied Energy 165 (2016) 345–356.
[39] Olivieria L, Caamano-Martina E, Olivierib F, Neila J. Integral energy performance characterization of semitransparent photovoltaic elements for building integration under real operation conditions. Energy and Buildings 2014; 68: 280–291.
[40] Yoon JH, Song JH, Lee SJ. Practical application of building integrated photovoltaic (BIPV) system using transparent amorphous silicon thin-film PV module. Sol Energy 2011;85:723–33.
[41] Peng JQ, Lu L, Yang HX. An experimental study of the thermal performance of a novel photovoltaic double-skin facade in Hong Kong. Sol Energy 2013;97:293–304.
[42] Peng JQ, Lu L, Yang HX, Ma T. Comparative study of the thermal and power performances of a semi-transparent photovoltaic façade under different ventilation modes. Appl Energy 2015;138:572–83.

[43] Jinqing Peng, Dragan C Curcija, Anothai Thanachareonkit, Eleanor S Lee, Howdy Goudey, Stephen E Selkowitz. Study on the overall energy performance of a novel c-Si based semitransparent solar photovoltaic window. Applied Energy 2019; 242: 854-872.

[44] Jinqing Peng, Dragan C Curcija, Anothai Thanachareonkit, Eleanor S Lee, Howdy Goudey. Energy Savings from PV-Integrated Window Glazing. The 2019 Buildings XIV International Conference

[45] Wienold J., J. Christoffersen (2006). Evaluation methods and development of a new glare prediction model for daylight environments with the use of CCD cameras. Energy and Buildings 38(7): 743-757.